Fatigue Analysis of Mechanically Fastened Joints Utilizing PSD Loads

Bharat M. Shah* and J. L. Russ†
Lockheed-Georgia Co., Marietta, Ga.

Multicomponent wing load and corresponding derived internal stress time histories are evaluated considering load transfer through mechanically fastened joints. These time histories are from both analytically derived and dynamic response test measured data considering flights through continuous turbulence of a heavy logistics aircraft. This evaluation is used as a basis to develop a rational fastener load transfer fatigue analysis methodology that includes gust loads in the power spectral density form. The technique developed includes the establishment of a matrix of axial-shear stress phasing relationships based on variations in operational flight parameters. The results of a durability assessment, utilizing the developed procedure, of specific structural joints subjected to two different load spectra are presented. Significant elements of this procedure are the aforementioned stress phasing relationships, joint geometric configuration data, fastener characteristics, and "built-up" S-N data. The results are compared to a fatigue assessment based on a uniaxial-stress fatigue analysis procedure. The potential applications of the developed load transfer analysis technique include structural joint design optimization and the durability evaluations of structural joints that have operating loads different from their design loads.

Introduction

IT is common knowledge that mechanically fastened joints are a major source of fatigue cracking in aircraft structure. In the design of structural joints, high strength materials and fastener systems have been exploited to design statically efficient joints. But, until the last 10-15 years, fatigue requirements were nonexistent, hence minimal attention, except maybe that of an esoteric nature, was directed toward evaluating the fatigue capability (durability) of such joints in the design phase. Since the conventional uniaxial-stress fatigue analysis method is unsuitable for the design of joints where interaction of axial, bearing, and shear stresses occur, the durability design of a particular joint has been developed by test or, perhaps by a handbook of successful practices, or a combination of both. The results of such tests are really only applicable to a specific spectra, which in general, has a fixed shear-bending-torsion external loads relationship.

Recently, interest concerning the incorporation of some form of "Load Alleviation System" on in-service aircraft to achieve structural load reduction for both static alleviation and durability enhancement has resulted in significant changes in external loading characteristics relative to design.[1] A passive lift distribution control system (PLDCS) provides reduced wing steady-state load by incorporating a constant, symmetric, uprigged aileron null position. An active lift distribution control system (ALDCS) provides reduced wing incremental bending moments through modification of the wing spanwise additional lift distribution by employing symmetric aileron deflection. However, aileron deflection also results in significant changes to wing torsion. This change in spectral parameters must be evaluated to quantify the durability enhancement that can be attributed to a particular load alleviation system.

Presented at the AIAA/ASME/SAE 17th Structures, Structural Dynamics, and Materials Conference, King of Prussia, Pa., May 5-7, 1976 (in bound volume of Conference papers, no paper number); submitted May 27, 1976; revision received April 18, 1977.

Index categories: Structural Design (including Loads); Structural Durability (including Fatigue and Fracture).

*Research, Design and Development Engineer. Associate Member AIAA.

†Group Engineer, Structural Analysis Department.

A load transfer fatigue analysis method has been developed,[2] which accounts for the interaction effects of discretely phased axial, bearing, and shear stresses in a mechanically fastened lap shear joint.

The discrete axial-shear stress relationship for maneuver incremental stresses is readily definable because normal maneuvering is a discrete quasistatic event. For dynamic load sources which are dependent on a power spectral density (PSD) method for describing the statistical variations of external loads, the corresponding internal axial and shear spectra in PSD form, are not time correlated due to the very nature of the statistical derivation.

The following load transfer fatigue analysis methodology utilizes analytically derived axial-shear stress time histories to empirically define phasing relationships. This phasing data is coupled with axial and shear stress PSD's, which, in turn, are used to define the cyclic variations of apparent tangential stress at the edge of a loaded fastener hole for a lap shear joint. Figure 1 is a schematic of the methodology development and correlation. The following sections provide a review of the load transfer method of analysis, development and correlation of analytic stress time histories, and durability evaluations of several lap shear joints for a heavy logistic aircraft subjected to different analytic gust spectra.

Load Transfer Analysis

Detailed knowledge about the local stress distribution around a loaded hole is of prime importance in the evaluation of a mechanically fastened joint designed to meet both a static and fatigue requirement. Jarfall[3] developed the stress severity factor (SSF) approach with the assumption of a linear influence of load transfer on the stress severity factor of lap axial joints. The empirical relation Jarfall proposed for the stress severity factor of the lap axial joint was expanded and modified by Cornell and Darby[2] for application to a lap shear joint. Shown in Fig. 2 are the stress components at the edge of a hole due to axial, bearing, and shear stresses as applied to a lap shear joint. The form of Cornell-Darby's equation to define the apparent local tangential stress at the fay surface edge of a fastener hole (f_{PK}) is

$$f_{PK} = \mathrm{FPI}(K_{TG} \cdot f_{ax} + K_{TB} \cdot \theta \cdot f_{br} + K_{TS} \cdot \tau)$$

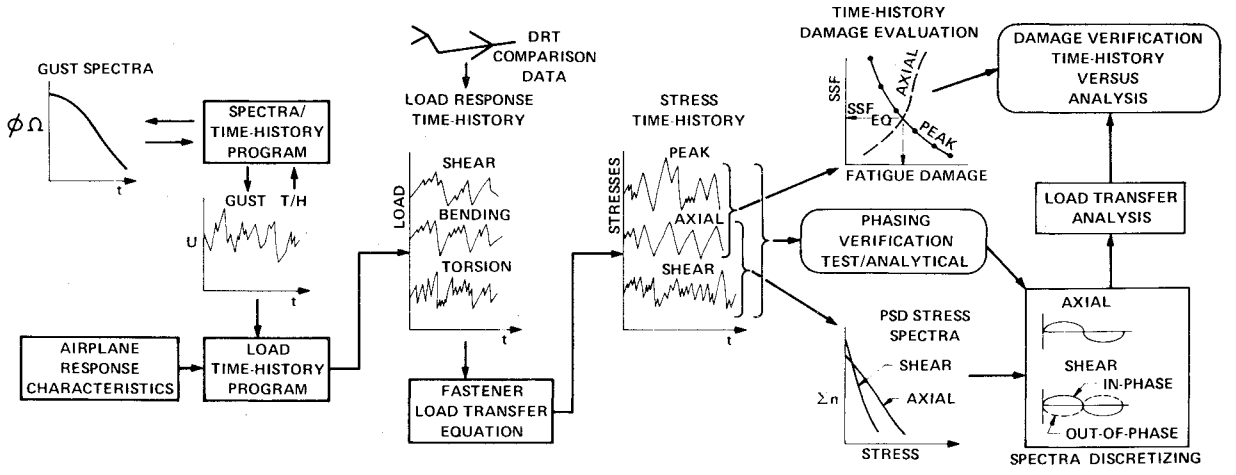

Fig. 1 Development and correlation – system flow diagram.

where

FPI = fastener performance index
f_{ax} = gross area uniaxial stress (psi)
f_{br} = uniform hole bearing stress (psi)
τ = gross area shear stress away from joint (psi)
K_{TG} = gross area uniaxial stress concentration factor
K_{TB} = hole bearing stress concentration factor
K_{TS} = gross area shear stress concentration factor
θ = tilt factor, ratio of peak to uniform hole bearing stress

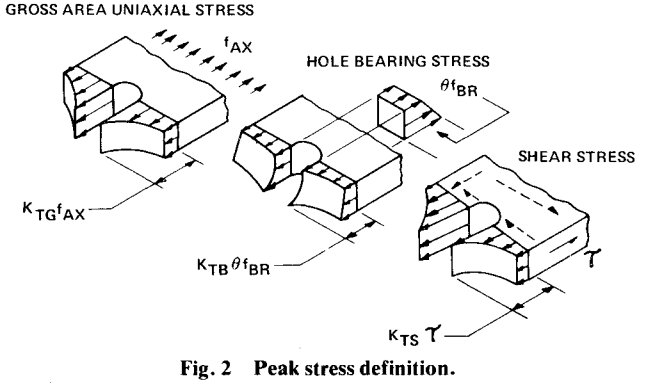

Fig. 2 Peak stress definition.

Fastener Performance Index (FPI)

The influence of hole preparation and installation on the local peak stress is identified by the FPI factor. A perfectly smooth hole with a "neat-fit" fastener installed is assumed to have a value of 1.0. Rough hole preparation will increase the FPI, whereas an interference fit fastener and/or clamp-up will reduce the FPI.

Figure 3 shows the configuration of component test specimens used to define the FPI of a specific fastener system.[4] This system consisted of a 60 deg countersunk head Titanium Taperlok with an aluminum collar installed in 7075-T6511 aluminum extrusions. A statistical evaluation of test results of 38 test specimens is also shown in Fig. 3 in terms of probability of survival (P_s) vs 1/FPI. The data is shown at two confidence levels, 50 and 95%.

Analysis/Test Correlation

Subsequent to the analysis/test correlation documented by Cornell and Darby,[2] additional load transfer fatigue analysis correlation has been evaluated through further comparisons of analysis to test results. Two box-beam-type specimens, approximately 2×2×5 ft, were flight-by-flight cyclic tested. These specimens represented a lap shear joint on a wing lower surface.[5] Each box-beam specimen was tested to a substantially different axial/torsion spectrum, hereafter identified as Spectrum I for box beam 4 and Spectrum II for box-beam 5. The magnitude of Spectrum II relative to Spectrum I

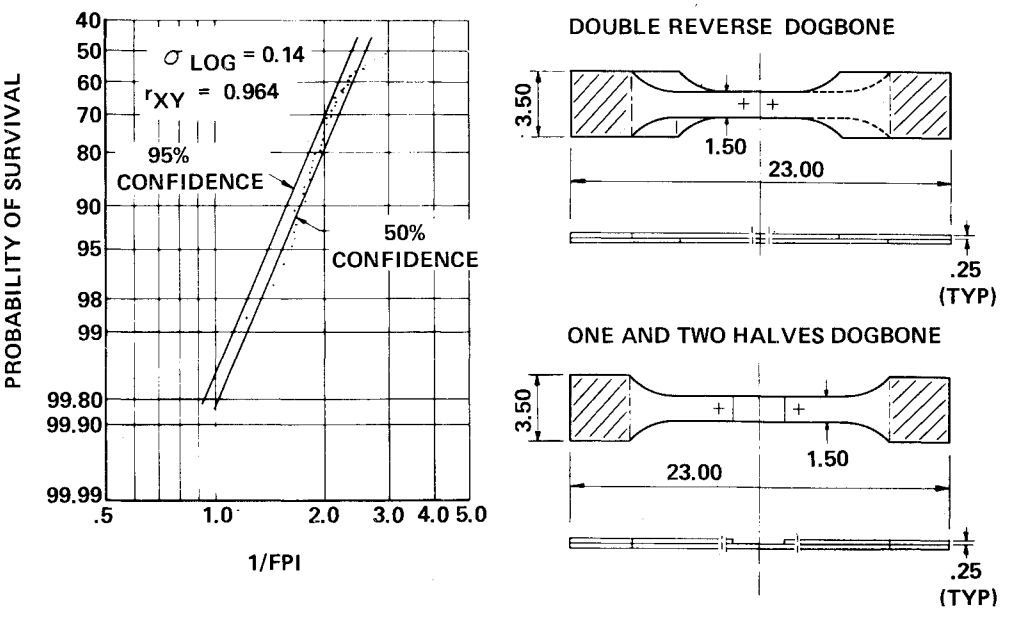

Fig. 3 Statistical evaluation of FPI.

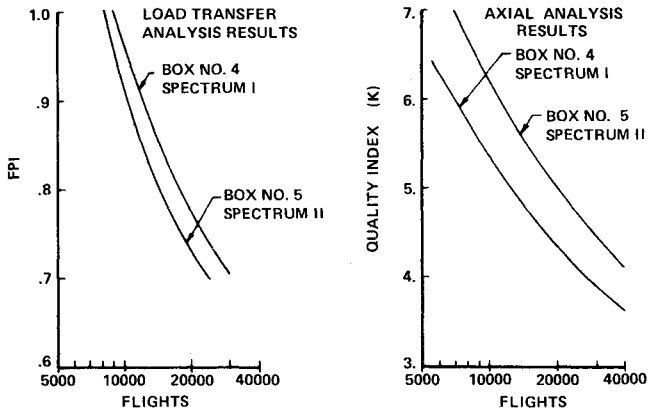

Fig. 4 Box-beam analysis results.

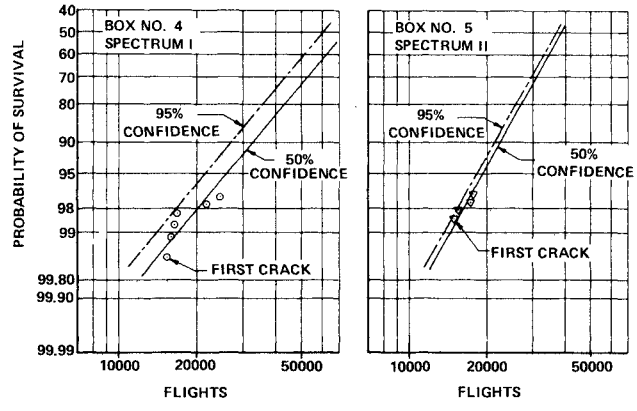

Fig. 5 Box-beam test results.

was established such that the varying axial stress was reduced approximately 50%, the varying shear stress was increased approximately 20%, and the axial-shear stress phasing was reversed. The mean stresses were not altered.

The load transfer analytical projections in terms of FPI versus flights is shown in Fig. 4. Also shown in Fig. 4 are the results of axial analyses based on notched coupon *S-N* data as a function of parametric quality index (K). Figure 5 shows the box-beam test results. The statistical evaluation of the test results of each specimen was performed subsequent to normalizing the results for crack length between 0.1 and 0.4 in. There were 240 similar fastener locations in each box-beam. The first six cracks from box-beam 4 and the first four cracks from box-beam 5 were used to statistically evaluate "initial-cracking" on the box-beam specimens. Comparative durability evaluations between the load transfer fatigue analysis projections, the axial fatigue analysis projections, and the box-beam flight-by-flight test results are presented in Table 1. The probabilities of survival for the first and fourth crack, at a 95% confidence level, were determined from the data in Fig. 5 for box-beam 4. The test results for box-beam 5 were also determined from Fig. 5 for the same probabilities. The load transfer analysis projections were determined from Fig. 4 using the FPI data from Fig. 3 at the probability of survival and confidence level based on box-beam 4.

For the axial analysis, the first and fourth cracks from box-beam 4 were considered as baseline, and the quality index K corresponding to their respective test flights was determined from the data presented in Fig. 4. The projections for box-beam 5 were then determined from Fig. 4 based on these quality indices.

The comparison of load transfer and axial fatigue analysis projections relative to Spectra I and II as shown in Fig. 4 are contradictory with respect to methods of analysis. The axial fatigue analyses show marked improvements in fatigue life (durability) for Spectrum II. However, the influence of

Table 1 Correlation of analysis and test results

BOX-BEAM SPECIMEN (SPECTRUM)	TEST RESULTS CRACK NO.	TEST RESULTS FLIGHTS ①	ANALYSIS LOAD TRANSFER P_C = 95% P_s[a]	ANALYSIS LOAD TRANSFER P_C = 95% FPI (FIG. 3)	ANALYSIS LOAD TRANSFER P_C = 95% FLIGHTS ②	ANALYSIS AXIAL K[b]	ANALYSIS AXIAL FLIGHTS ③	CORRELATION LOAD TRANSFER ②/①	CORRELATION AXIAL ③/①
4(I)	1	14,100			13,400	BASELINE		0.95	—
			98.7	.875					
5(II)		13,800			11,500	4.90	22,000	0.83	1.60
4(I)	4	15,500			16,000	BASELINE		1.03	—
			98.0	.830					
5(II)		14,500			13,100	4.22	36,000	0.90	2.48

[a] Probability of survival. [b] Based on specimen 4(*I*) test results.

Table 2 Operational parameters of DRT flights

FLIGHT NO.	CONFIG.	GROSS WEIGHT (KIPS)	FUEL (KIPS)	CARGO (KIPS)	VELOCITY (KEAS)	ALTITUDE (FT.)	σGUST (F.P.S.)
342	PLDCS	517	103	90	326	6,850	8.66
342	ALDCS	510	96	90	326	7,017	7.71
349	PLDCS	678	244	110	325	6,510	7.89
349	ALDCS	682	248	110	329	6,430	6.44
350	PLDCS	615	181	110	322	14,980	7.30
350	ALDCS	602	168	110	325	15,050	7.21
352	PLDCS	490	78	88	318	20,790	4.33
352	ALDCS	490	84	88	321	20,970	4.82

bearing stresses accounted for in the load transfer analysis indicates that Spectrum II is more critical than Spectrum I. The axial-shear phasing relationships in Spectrum II for the PSD gust load sources were completely opposite to that of Spectrum I. This comparison illustrates the dilemma in extending the test results from one loads spectrum to another which have different component relationships.

The results in Table 1 verify/demonstrate two major points, namely: 1) coupon test derived FPI's can be utilized for full-scale specimen evaluation; and 2) the scatter in durability estimated with the load transfer analysis is considerably smaller than it is with the conventional, uniaxial-stress fatigue analysis.

Development of PSD Analysis Procedure

The subsequent parts of this paper are directed toward the use of gust load/stress time history data to determine properly phased stress input to the load transfer durability evaluation.

Development of Analytical Time Histories

In the absence of a wide parametric range of flight-test-measured gust load/stress time histories, the logical approach is to resort to the development of analytically generated time histories for defined flight conditions. To provide economical analytic gust load time histories, a fast fourier transform (FFT) digital filter technique has been developed.[6] This procedure was developed to provide multicomponent load spectra data compatible with current dynamic loads analysis procedures,[7] i.e., with respect to RMS response (σ) and characteristic frequency (N_0). It was also necessary that the analytically generated time histories be representative, from a load transfer standpoint, of the dynamic response test (DRT) measured data. Table 2 identifies the DRT flights and operational parameters that were used as check cases. Load time histories of shear, bending, and torsion are generated by employing a FFT technique to filter input gust intensity time histories with load response transfer functions representing the linear system. Analytical gust time histories are generated as a stationary and Gaussian random process having the characteristics of the von Karman spectrum. The load response functions are derived from a theoretical model of the aircraft and also by cross-spectral analysis of measured response time histories with measured gust component time histories. The primary features and reasons for the efficiency of the FFT processing method are: 1) the transfer function is converted to a frequency filter which allows a larger interval

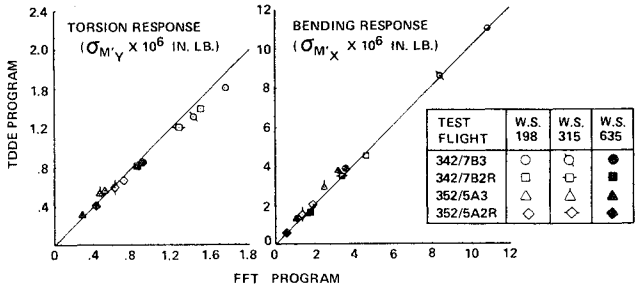

Fig. 6 Loads response comparisons.

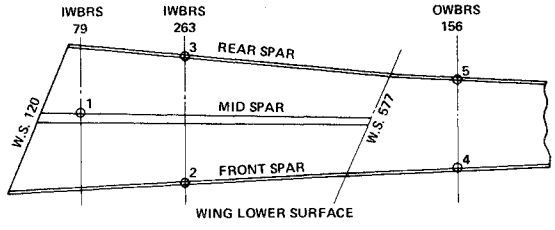

ANALYSIS POINT	JOINT DATA									
	FASTENER DATA					PANEL DATA				
	DIA.	HEAD	SPACING	PITCH	MAT'L	ROWS	T_1	T_2	T_2'[a]	θ
1	.3125	CSK	1.08	–	STL	1	.250	.250	.218	1.167
2	.2500	CSK	1.01	–	TI	1	.200	.200	.151	1.340
3	.2500	CSK	1.25	.68	TI	2	.260	.260	.211	1.838
4	.2500	CSK	1.15	–	TI	1	.265	.265	.215	1.874
5	.2500	CSK	1.03	1.00	TI	2	.260	.260	.210	1.823

[a] $T_2' = T_2 - .5$ (CSK DEPTH)

Fig. 7 Analysis locations and configurations.

between time points; and 2) it permits the filtering operation to be accomplished simply by multiplying the transform of the input time history with the frequency filter.

The comparison of individual component load spectra for wing loads from the FFT program and the current time-history dynamic loads analytic procedure, i.e., a time domain differential equation (TDDE) program, was performed for the test flights. Shear, bending, and torsion rms responses from the FFT program were approximately within 10% of the TDDE results at three wing locations.

Figure 6 shows a spanwise bending moment and torsion response comparison of data from the FFT/TDDE programs. The correlation is considered to be acceptable.

Fatigue Analysis Locations

The analyses of shear, bending, torsion load time histories of eight flight conditions were performed at five analysis points on the wing lower surface panel-to-panel joints. The surface panels are machined from 7075-T6511 aluminum extrusion and the splices utilize 60 deg countersunk titanium TaperLok fasteners with aluminum collars. The load transfer analysis is performed at the fay surface for the countersunk panel. Figure 7 shows the location and joint data for the analysis points.

Definition of Axial-Shear Phasing Relationship

The test measured and corresponding analytically derived shear, bending, torsion load time histories were converted to internal stress time histories by utilizing linear stress-to-load relationships. As illustrated in Fig. 8, the apparent tangential stress time history at the edge of the hole is defined on a discrete time basis (i.e., every 0.025 sec) from the shear and axial stress time histories.

The phasing relationship of the axial-shear stress is defined as the product of the axial-shear stress sense relative to their respective mean stresses. The stress reversals at the edge of a loaded hole caused by the axial and shear stresses are evidenced by fluctuations of the peak stress. From the standpoint of joint fatigue, the local peak stress cycle

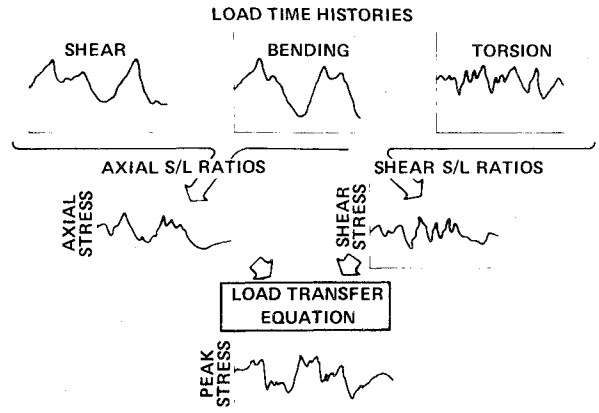

Fig. 8 Typical stress time-history generation.

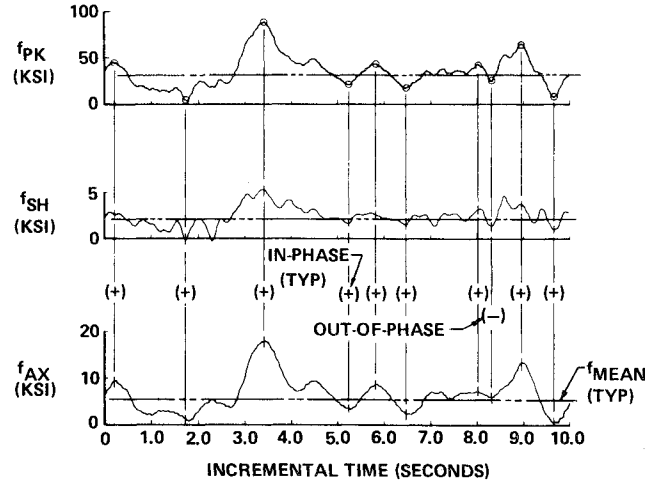

Fig. 9 Definition of stress phasing relationship.

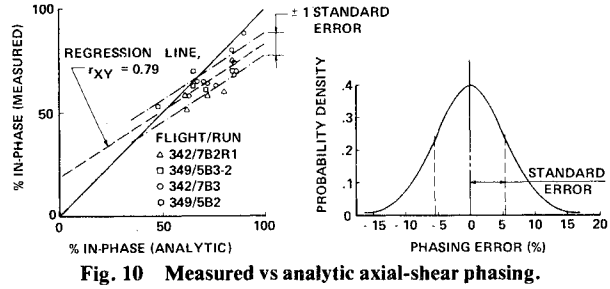

Fig. 10 Measured vs analytic axial-shear phasing.

variations are of prime importance. Hence, for the time at which the peak varying stress is a maximum (or minimum) during each half cycle, the instantaneous relationship between axial and shear stress amplitude is categorized. They are in-phase if both stresses have the same sense relative to their mean and out-of-phase if they have opposite sense relative to their mean. Figure 9, based on measured DRT data, illustrates the definition of the axial-shear stress phasing relationship relative to the cyclic variation of peak stress.

Figure 10 shows comparative measured versus analysis results of axial-shear phasing relationships derived from stress histories of four measured DRT flights utilizing the procedure as explained above. As can be seen, the results indicate acceptable correlation with measured time-history data. The phasing standard error is approximately ±5% between the measured and analytically derived time histories for similar DRT flights.

Evaluation of Stress Phasing Approach

The application of the developed axial-shear stress phasing relationships is evaluated by comparing calculated load

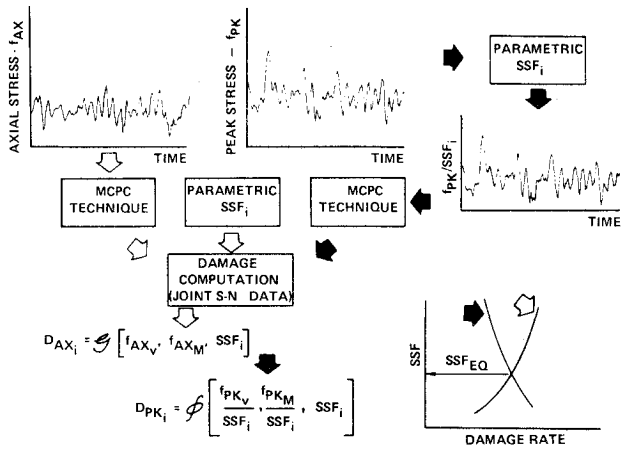

Fig. 11 Time-history analysis procedure.

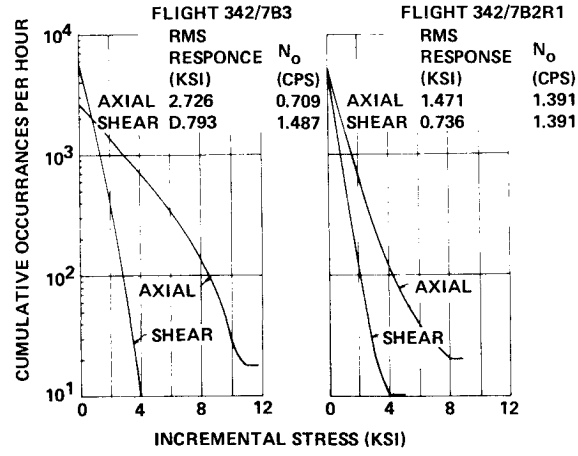

Fig. 12 PSD stress spectra.

transfer fatigue damages computed from the measured load/calculated stress time histories with damage computed from the conversion of those same stress histories to PSD's in the form of rms response (σ), characteristic frequency (N_0), and the associated phasing relationships.

Four test flights and three spanwise splice analysis points were utilized for this evaluation. Figure 11 illustrates the load transfer damage computation procedure from the axial and peak stress time histories.

Time-History Fatigue Damage Analysis

The cycle definition from the stress time history is generated utilizing the mean crossing peak count with floating mean method, identified here as MCPC technique. With this technique, the mean at any discrete time is identified by the average of the stresses of a finite (20) number of max/min values preceding and following the specific time cut. The max/min stresses are refined to exclude significantly biased stresses caused by higher (lower) local peaks. A stress cycle is defined as the maximum range between two consecutive mean crossing with a positive slope. The axial and peak stress time histories are peak counted in terms of the number of cycles in uniform mean and varying stress ranges. The accumulated damage due to the axial mean and variable stress range was computed (Miner's linear cumulative damage hypothesis) for several parametric SSF's. The peak mean and variable stresses are considered as elastic local stresses; hence, for damage computation, equivalent "far-field" axial stress is defined based on the assumption of a linear relationship between local and far-field stress. This is accomplished by dividing the peak mean and variable stress by the same SSF's utilized in the axial analysis. Then damage was computed for the specific SSF and the far-field axial mean and variable stresses. The intersection of SSF vs damage rate for the axial and peak stress calculations (Fig. 11) defines the equivalent SSF (SSF_{EQ}) and the load transfer fatigue damage rate for the time history being investigated. The results of these computations are presented in Table 3.

Table 3 Comparison of durability evaluation

ANAL. POINT	FLIGHT NO.	PSD SPECTRA DESCRIPTION σ_{AX} (KSI)	$N_{o\,AX}$ (CPS)	σ_{SH} (KSI)	$N_{o\,SH}$ (CPS)	$N_{o\,PK}$ (CPS)	f_{AX} f_{SH} IN PHASE RELATIONSHIP (PER CENT)	DAMAGE RATE X 10^3 TIME HISTORY ①	f_{AX} : f_{SH} PHASING ②	DAMAGE RATIO ②:①
	342/7B3	2.56	.928	.823	1.489	1.05	64	.504	.584	1.158
	342/7B2R1	1.47	1.391	.736	1.391	1.391	58	.232	.259	1.116
2	349/5B32	2.72	.709	.791	1.487	.956	65	.630	.749	1.188
	349/5B22	1.81	.818	.766	1.355	1.011	61	.380	.346	0.910
	342/7B3	2.25	.888	.316	1.711	1.075	63	.280	.277	0.989
	342/7B2R1	1.30	1.380	.254	1.967	1.380	57	.108	.097	0.902
3	349/5B32	2.43	.719	.404	1.779	1.208	58	.232	.199	0.856
	349/5B22	1.60	.854	.423	1.437	1.322	53	.113	.106	0.893
	342/7B3	3.12	1.18	.845	1.605	1.008	71	.779	.869	1.106
	342/7B2R1	1.76	1.69	.775	1.381	1.649	58	.433	.432	0.998
4	349/5B32	3.66	.886	1.030	1.502	.969	65	.190	.157	0.797
	349/5B22	2.24	1.125	.803	1.512	1.089	63	.804	.930	1.156

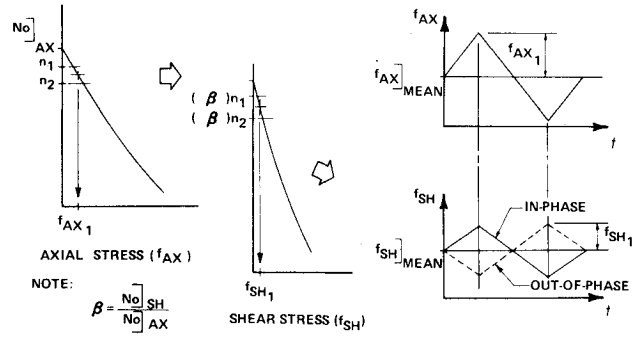

Fig. 13 PSD stress spectra segmentation.

PSD Stress Spectra Fatigue Damage Analysis

The axial and shear stress spectra of the four test flights were converted to independent PSD spectra in the form of rms response and characteristic frequencies. Table 3 shows the spectra description of each time history and the axial-shear stress phasing relationships defined from the time-histories utilized in the damage computation. Figure 12 is a typical incremental shear and axial stress spectra generated from the axial-shear stress time histories of two of the test flights.

The axial incremental stress spectrum was divided into several constant stress interval bands. The mid-value stress of each band and the applied number of cycles at this stress is defined by taking the difference in cumulative occurrence of the two extremities of each stress band. Since bending constitutes the dominant stress on the aircraft wing, axial stress frequencies are assumed dominant. To define the magnitude of shear stress amplitude corresponding to each axial stress cycle, the assumption was made that the relative magnitude of axial and shear stresses are compatible. In other words, the smaller axial stress magnitudes "go with" the smaller shear stress magnitudes, and so on. In order to define the amplitude of shear stress corresponding to the defined axial stress, the shear stress occurrence curve is subdivided into the same number of bands as the axial stress data. These bands are constructed such that they are proportional to the frequency ratio (β). Frequency ratio is defined as the ratio of the shear stress characteristic frequency (N_0) to the axial stress characteristic frequency. The mid-value shear stress of each band is associated with the corresponding axial stress amplitude.

Figure 13 illustrates the procedure for segmenting the incremental stress spectra into discrete bands as related to axial-shear stress magnitudes and stress phasing. The number of cycles in each band is distributed in proportion to the percent in-phase and out-of-phase and is utilized in conjunction with the associated magnitudes of axial and shear stress to

Table 4 Parametric grid of stress phasing relationships

PARAMETRIC GRID			POINT 2 $f_{AX} \cdot f_{SH}$ IN-PHASE	PARAMETRIC GRID			POINT 2 $f_{AX} \cdot f_{SH}$ IN-PHASE
MACH/ ALTITUDE	FUEL (KIPS)	CARGO (KIPS)	RELATION (PER CENT)	MACH/ ALTITUDE	FUEL (KIPS)	CARGO (KIPS)	RELATION (PER CENT)
.233/1500	94.25	20.	75.5	.233/1500	94.25	160.0	70.2
.233/1500	214.50	20.	83.2	.233/1500	214.50	160.0	80.6
.453/10000	94.25	20.	68.7	.453/10000	94.25	160.0	84.5
.453/10000	214.50	20.	66.4	.453/10000	214.50	160.0	83.4
.775/30000	94.25	20.	77.3	.775/30000	94.25	160.0	84.2
.775/30000	214.50	20.	71.9	.775/30000	214.50	160.0	77.5

$f_{AX} \cdot f_{SH}$ IN-PHASE RELATIONSHIP BY GUST SOURCE - ANALYSIS POINT 2

SOURCE	PERCENT	SOURCE	PERCENT	SOURCE	PERCENT	SOURCE	PERCENT
CLIMB	76	CRUISE	78	DESCENT	77	TRAFFIC	77

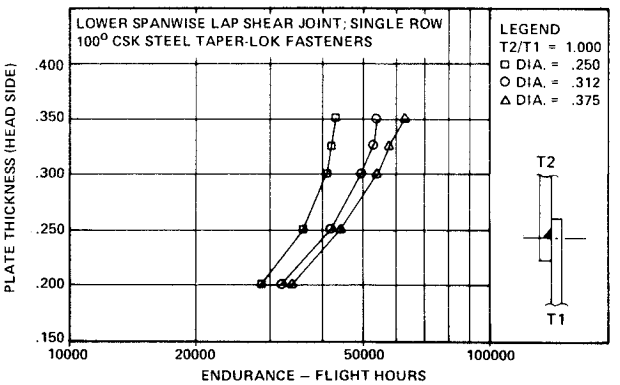

Fig. 14 Typical structural joint design evaluation.

calculate the peak stress. The computation of the equivalent stress severity factor and damage rate for each stress interval is calculated independently for in-phase and out-of-phase stresses and summed.

Table 3 summarizes the results of this durability evaluation. Since the load transfer calculated fatigue damage from the stress time histories are computed on a cycle-by-cycle basis, the characteristic frequency of the peak stress time histories is inherent in the time-history computed damages. As stated previously, the gust stress spectrum for analysis considered that the axial stress characteristic frequency is dominant, therefore, for a valid damage comparison, the time-history generated damages were modified by the ratio of axial to peak stress characteristic frequencies.

The durability evaluation demonstrates a reasonable correlation of this rational approach, that is, to utilize analytically generated time histories to define axial-shear stress phasing relationships for load sources that are defined in PSD form.

Application

In addition to accounting for the interaction effects of axial, shear, and bearing stresses, the load transfer fatigue analysis is virtually spectra independent. With the axial-shear stress phasing relationships available for load sources defined in the PSD form, a joint load transfer fatigue analysis and/or joint optimization for any set of missions can be performed. For a service missions analysis, the parametric axial-shear stress phasing relationships defined from the gust load time histories grid data can be assigned to specific mission segments on a similarity of conditions basis.

Table 4 shows the parametric flight grid conditions for which axial-shear stress phasing relationships have been derived, and also the derived phasing relations for an analysis point. The average axial-shear stress phasing relationships for the operational range of fuel and cargo weights at selected speed/altitude combinations are calculated and utilized for the mission segments representing climb, cruise, descent, or traffic.

A joint optimization load transfer fatigue analysis of a wing lower surface lap shear joint has been performed. A UNIVAC 1106 computer program[8] was developed to execute this analysis. The results are illustrated in Fig. 14 for the fastener head-side surface panel of the joint. The type of analysis illustrated in Fig. 14 could significantly aid in the design of structural joints. It serves as an analysis tool to maintain control of operating fastener bearing stresses. For example, a joint could be made bearing critical simply by increasing the strength of the fastener. This would result in higher operating bearing stresses. For joints designed primarily by static considerations, this could be an acceptable solution. However, to achieve desired fatigue durability goals, it may be necessary to reduce the bearing stresses. This procedure provides a trade-off tool between a higher strength fastener with lower weight and lower operating bearing stresses for durability.

Conclusions

As a result of the development and analysis that have been presented, the following conclusions have been reached.

1) The method developed for defining the axial-shear phasing is a rational approach with which the quantitative durability predictions of different PSD spectra can be made utilizing the load transfer method of fatigue analysis. It is demonstrated that analytic predictions by the load transfer method of fatigue analysis correlates very well with the test results.

2) With the analysis method developed here, it is possible during initial design to optimize the joint design configuration with respect to weight, cost, and strength in order to achieve a more balanced design, meeting both static and fatigue requirements.

Acknowledgment

The majority of investigative effort was funded through the C-5 System Program Office, Wright-Patterson Air Force Base, Ohio, under several Air Force contracts.

References

[1] Disney, T. E., "The C-5A Active Load Alleviation System," AIAA Paper 75-991, Aug. 1975.

[2] Cornell, B. L. and Darby, L. G., "Correlation of Analysis and Test Data To The Effect of Fastener Load Transfer on Fatigue," AIAA Paper 74-983, Aug. 1974.

[3] Jarfall, J. E., "Optimum Design of Joints: Stress Severity Factor Concept," *5th I.C.A.F. Symposium, Fatigue – Design, Operational and Economics Aspects*, Melbourne, Australia, May 1967.

[4] Lockheed-Georgia Company, "Statistical Reduction of Element Data – Empirical Constant Determination," LSR 7114-73-0270, May 1973.

[5] Cornell, B. L., Shah, B. M., and Lantzy, J. H., "C-5A ALDCS Structural Fatigue Evaluation," Lockheed-Georgia Company, Marietta, Ga., LG1US48-2-8, May 1975.

[6] Shah, B. M., Allen, H. D., and Cohen, L. R., "Analysis of Mechanically Fastened Joints Utilizing PSD Loads – Technique Development and Application," Lockheed-Georgia Company, Marietta, Ga., LG75ER0067, October 1975.

[7] Jones, F. L., "C-5A Dynamic Response to Abrupt Maneuvers," Lockheed-Georgia Company, Marietta, Ga., LG1US44-1-10, Sept. 1967.

[8] Shah, B. M., "A User's Manual For Joint Optimization and Residual Stress Analysis Program," Lockheed-Georgia Company, Marietta, Ga., SMN 388, Nov. 1977.